

Singlet C₂H₂Li₂: Acetylenic and 1,2-Dilithioethene Isomers. A Remarkably Congested Potential Energy Hypersurface for a Simple Organometallic System

Evan E. Bolton,^{*†} William D. Laidig,^{*‡} Paul von Ragué Schleyer,^{*†§} and Henry F. Schaefer, III[†]

Contribution from the Center for Computational Quantum Chemistry, University of Georgia, Athens, Georgia 30602, Miami Valley Laboratories, The Procter & Gamble Company, P.O. Box 398707, Cincinnati, Ohio 45239-8707, and Computer Chemistry Center, Institut für Organische Chemie I, Universität Erlangen-Nürnberg, Henkestrasse 42, D-91054 Erlangen, Germany

Received March 7, 1994[⊙]

Abstract: The potential energy surface (PES) for the singlet 1,2-dilithioethene and acetylenic C₂H₂Li₂ isomers was carefully surveyed using *ab initio* quantum mechanical methods. Three previously unreported minima (including, remarkably, the global minimum) were located, a planar, monobridged *trans*-1,2-dilithioethene and two acetylenic structures. A total of seven minima and ten transition states for interconversion of minima were investigated (seven transition states are reported here for the first time). Vibrational frequencies were evaluated for all structures through the coupled-cluster method including all single and double excitations with a double- ζ plus polarization basis set (CCSD/DZP). An acetylenic isomer (**11**), namely, a C_s complex between lithioacetylene and LiH, is the global minimum on the C₂H₂Li₂ PES. This was 34 kcal/mol more stable at CCSD/DZP (+ZPVE) than the two lowest lying singlet 1,2-dilithioethene structures, a *trans* planar C_{2h} form with acute CCLi angles (**1**) and a *cis* doubly bridged C_{2v} structure (**5**). The other singlet 1,2-dilithioethene minima, *cis* planar monobridged C_s (**14**), *cis* planar dibridged C_{2v} (**3**), and *trans* planar monobridged C_s (**7**), are 4.3, 8.4, and 19.4 kcal/mol higher lying than **1** at CCSD/DZP (+ZPVE), respectively. The carbon-lithium bonding is ionic in character in all these species.

Introduction

The seeming simplicity of dilithioethene is deceptive.¹⁻⁶ Theoretical studies reveal numerous low-lying minima for singlet 1,2-dilithioethene, most of which are quite unusual. Unfortunately, most of these computational predictions have not been verified as experiments on dilithioethene are complicated, e.g., by aggregation.⁷

The first recorded attempt to prepare 1,2-dilithioethene, by transmetalation of a distannyl derivative, was unsuccessful.⁸ However, Maercker, Graule, and Demuth (MGD)⁹ used mercury precursors and characterized *cis*- and *trans*-1,2-dilithioethene as reaction products with dimethyl sulfate and with bromine. A *cis*-*trans* rearrangement of 1,2-dilithioethene did not occur. It was proposed,⁹ however, that *cis*-1,2-dilithioethene will decompose into lithium hydride and lithioacetylene. Previous *ab initio* results⁴ dealt only with isolated species, but predicted that the elimination of lithium hydride should proceed endothermically and should be less favorable than the elimination of H₂ or Li₂. MGD were unable to detect any H₂ or Li₂ and proposed, therefore, that the

Table 1. Summary of the Relative Energy (kcal/mol) Predictions of Apeloig, Clark, Kos, Jemmis, and Schleyer^a and of Schleyer, Kaufman, Kos, Clark, and Pople (SKKCP)^b for the 1,2-Dilithioethene Molecule

structure ^c	symmetry	level of theory			imaginary frequencies ^e
		RHF/ 3-21G	RHF/ 6-31G*	MP2/ 6-31G*/RHF ^d	
0	D _{2h}	48.9	54.2		2
1	C _{2h}	0.0	0.0	0.0	0
2	C _s	24.2	26.6	22.7	1
3	C _{2v}	13.4	11.5	10.1	0
4	C _s	15.4	14.0	14.1	1
5	C _{2v}	-2.3	1.7	0.9	0
14	C _s	3.1	6.2	7.2	0
15	C _{2v}	16.7	20.0	21.9	1

^a See ref 4. ^b See ref 5. ^c Structures may be viewed in Figure 1. ^d MP2/6-31G* single point energy at the RHF/6-31G* optimized geometry. ^e The absence of imaginary vibrational frequencies denotes a minimum. One imaginary frequency denotes a transition state. Two imaginary frequencies denote a higher order saddle point.

lithioacetylene and lithium hydride products form a relatively stable mixed complex, and this helped drive the elimination reaction.

Manceron and Andrews¹⁰ have provided the only experimental spectroscopic data on dilithioethene. They simultaneously codeposited atomic lithium atoms and acetylene in argon matrices at 15 K. On the basis of isotopic labeling, the resulting IR spectra were assigned to four species with different compositions. Three fundamental frequencies, assigned to C₂H₂Li₂, were consistent with an acute CCLi angle and pointed to a lithium bridged structure.

In 1980, Apeloig, Clark, Kos, Jemmis, and Schleyer (ACKJS)⁴ reported the first theoretically predicted singlet 1,2-dilithioethene structures. These were reexamined in a later survey by Schleyer, Kaufmann, Kos, Clark, and Pople (SKKCP).⁵ Harmonic

(10) Manceron, L.; Andrews, L. *J. Am. Chem. Soc.* **1985**, *107*, 563-568.

[†] University of Georgia.

[‡] The Procter & Gamble Co.

[§] Universität Erlangen-Nürnberg.

[⊙] Abstract published in *Advance ACS Abstracts*, September 15, 1994.

(1) Apeloig, Y.; Schleyer, P. R.; Binkley, J. S.; Pople, J. A. *J. Am. Chem. Soc.* **1976**, *98*, 4332-4334.

(2) Nagase, S.; Morokuma, K. *J. Am. Chem. Soc.* **1978**, *100*, 1661-1666.

(3) Laidig, W. D.; Schaefer, H. F. *J. Am. Chem. Soc.* **1979**, *101*, 7184-7188.

(4) Apeloig, Y.; Clark, T.; Kos, A. J.; Jemmis, E. D.; Schleyer, P. R. *Isr. J. Chem.* **1980**, *20*, 43-50.

(5) Schleyer, P. R.; Kaufmann, E.; Kos, A. J.; Clark, T.; Pople, J. A. *Angew. Chem., Int. Ed. Engl.* **1986**, *25*, 169-170.

(6) Ritchie, J. P.; Bachrach, S. M. *J. Am. Chem. Soc.* **1987**, *109*, 5909-5916.

(7) Wakefield, B. J. *The Chemistry of Organolithium Compounds*; Pergamon Press: New York, 1974.

(8) Seyferth, D.; Vick, S. C. *J. Organomet. Chem.* **1978**, *144*, 1-12.

(9) Maercker, A.; Graule, T.; Demuth, W. *Angew. Chem., Int. Ed. Engl.* **1987**, *26*, 1032-1034.

Table 2. Results for the Lithium Dimer, Li₂, in D_{∞h} Symmetry^a

level of theory	RHF/6-31G**	MP2/6-31G**	RHF/DZP	CISD/DZP	CCSD/DZP	experiment ^b
total energy	-14.866 925	-14.886 849	-14.869 264	-14.911 961	-14.913 449	
bond length (Li-Li)	2.807	2.773	2.806	2.733	2.730	2.673
ω(Li-Li stretch (σ _g)) (cm ⁻¹)	340	339	335	334	332	351

^a The harmonic vibrational frequency ω is listed along with the energy (hartrees) and bond length (Å). ^b Huber, K. P.; Hertzberg, G. *Constants of Diatomic Molecules*; Van Nostrand Reinhold Co.: New York, 1979.

Table 3. Results for Lithium Hydride in C_{∞h} Symmetry^a

level of theory	RHF/6-31G**	MP2/6-31G**	RHF/DZP	CISD/DZP	CCSD/DZP	experiment ^b
total energy	-7.981 340	-8.002 197	-7.982 205	-8.017 831	-8.018 047	
dipole moment	5.95	5.79	5.95	5.73	5.72	5.88 ^c
bond length (Li-H)	1.630	1.623	1.621	1.621	1.621	1.594
ω(Li-H stretch (σ)) (cm ⁻¹) (intensity (km/mol))	1420 (195.3)	1412 (157.2)	1432 (161.1)	1367 (98.7)	1364 (95.9)	1406 (-)

^a The harmonic vibrational frequency ω and infrared intensity are listed along with the energy (hartrees), dipole moment (D), and bond length (Å). ^b Huber, K. P.; Hertzberg, G. *Constants of Diatomic Molecules*; Van Nostrand Reinhold Co.: New York, 1979. ^c Nelson, R. D.; Lide, D. R.; Maryott, A. A. *Selected Values of Electric Dipole Moments for Molecules in the Gas Phase*; NSRDS-NBS10; U.S. Department of Commerce, U.S. Government Printing Office: Washington, DC, 1967.

Table 4. Results for Linear Lithioacetylene in C_{∞h} Symmetry^a

level of theory	RHF/6-31G**	MP2/6-31G**	RHF/DZP	CISD/DZP	CCSD/DZP	experiment ^b
total energy	-83.694 064	-83.967 529	-83.707 131	-83.987 335	-84.011 944	
dipole moment	6.04	5.74	6.36	6.36	6.34	
bond length						
C ₁ -C ₂	1.210	1.242	1.215	1.235	1.243	
C ₁ -Li ₃	1.923	1.907	1.934	1.934	1.937	
C ₂ -H ₄	1.058	1.065	1.062	1.069	1.073	
ω (cm ⁻¹) (intensity (km/mol))						
C-H stretch (σ)	3615 (10.4)	3502 (9.0)	3603 (19.6)	3510 (12.7)	3456 (9.9)	
C-C stretch (σ)	2200 (22.6)	1946 (24.2)	2165 (8.7)	2043 (6.1)	1982 (5.4)	
C-C-H bend (π)	801 (65.9)	668 (57.4)	785 (91.5)	687 (83.7)	645 (83.0)	
C-Li stretch (σ)	673 (138.1)	667 (119.9)	654 (135.0)	640 (124.8)	631 (118.8)	
C-C-Li bend (π)	171 (120.2)	177 (113.3)	193 (126.7)	181 (119.0)	175 (115.7)	

^a The harmonic vibrational frequencies ω and infrared intensities are listed along with the energy (hartrees), dipole moment (D), and bond lengths (Å).

Table 5. Results for Linear Acetylene in D_{∞h} Symmetry^a

level of theory	RHF/6-31G**	MP2/6-31G**	RHF/DZP	CISD/DZP	CCSD/DZP	experiment
total energy	-76.821 837	-77.091 458	-76.831 521	-77.107 979	-77.131 015	
bond length						
C-C	1.186	1.217	1.191	1.212	1.221	1.204
C-H	1.057	1.062	1.062	1.068	1.072	1.062
ω (cm ⁻¹) (intensity (km/mol))						
C-H stretch (σ _g)	3697 (0.0)	3593 (0.0)	3674 (0.0)	3576 (0.0)	3524 (0.0)	3495 ^b (0.0)
C-H stretch (σ _u)	3586 (91.9)	3503 (87.4)	3570 (100.9)	3488 (84.5)	3440 (76.3)	3415 ^b (71 ± 2 ^c)
C-C stretch (σ _g)	2243 (0.0)	2003 (0.0)	2204 (0.0)	2074 (0.0)	2012 (0.0)	2008 ^b (0.0)
C-C-H bend (π _u)	877 (99.9)	755 (80.5)	857 (114.4)	767 (95.3)	733 (89.9)	747 ^b (175 ± 5 ^c)
C-C-H bend (π _g)	799 (0.0)	458 (0.0)	767 (0.0)	631 (0.0)	577 (0.0)	624 ^b (0.0)

^a The harmonic vibrational frequencies ω and infrared intensities are listed along with the energy (hartrees) and bond lengths (Å). ^b Strey, G.; Mills, I. M. *J. Mol. Spectrosc.* **1976**, *59*, 103. ^c Koops, T. A.; Smit, W. M.; Visser, T. *J. Mol. Spectrosc.* **1984**, *112*, 285.

vibrational frequency computations revealed that only some of the structures considered previously were minima. Additional singlet 1,2-dilithioethene structures were delineated and transition states interconverting the minima were located. The energy ordering of these stationary points is summarized in Table 1, and the structures are sketched in Figure 1. The three lowest lying energy candidates were a singlet planar distorted *trans* C_{2h} structure and two singlet *cis* forms, one a doubly bridged C_{2v} and the other a planar C_s distorted form, with a planar tetracoordinate carbon, structures **1**, **3**, and **14**, respectively, where the naming convention *trans* and *cis* corresponds, to the positions of the hydrogens relative to the C=C double bond regardless of the position of the lithiums.

These early computational explorations¹⁻⁵ stimulated experimental investigations.⁸⁻¹⁰ Conventionally prepared 1,2-dilithioethene derivatives have not been isolated but have been characterized through their chemical reactions, e.g., derivation of products with dimethyl sulfate. Experiments are complicated by the strong tendency of lithium compounds to aggregate in the solid state.⁷ However, matrix isolation studies may allow realization of some of the structures described here. The predicted vibrational spectra reported here should assist the interpretation of experimental findings.^{9,10} The present comprehensive theo-

Table 6. Weinhold Natural Charges,^a Computed at the MP2/6-31G** Level, for Lithioacetylene, Acetylene, Lithium Hydride, and All States Examined on the Singlet 1,2-Dilithioethene PES

structure ^b	C ₁	C ₂	Li ₃	Li ₄	H ₅	H ₆
LiC≡CH	-0.73	-0.34	0.86		0.21	
HC≡CH	-0.23	-0.23			0.23	0.23
LiH			0.69		-0.69	
1	-0.93	-0.93	0.82	0.82	0.10	0.10
2	-0.86	-1.06	0.83	0.80	0.02	0.27
3	-0.91	-0.91	0.82	0.88	0.06	0.06
4	-0.95	-0.95	0.89	0.76	0.12	0.12
5	-0.94	-0.94	0.75	0.75	0.18	0.18
6	-1.08	-0.54	0.67	0.72	0.18	0.04
7	-0.69	-0.41	0.13	0.61	0.20	0.15
8	-0.46	-0.39	-0.08	0.50	0.23	0.20
9	-0.25	-0.25	0.16	-0.18	0.27	0.27
10	-0.70	-0.85	0.84	0.89	-0.41	0.23
11	-0.45	-0.64	0.81	0.81	-0.77	0.23
12	-0.77	-0.30	0.81	0.81	-0.77	0.22
13	-0.71	-0.65	0.80	0.82	-0.49	0.23
14	-1.08	-0.76	0.75	0.80	0.17	0.11
15	-0.82	-0.82	0.67	0.67	0.15	0.15
16	-1.11	-0.78	0.82	0.74	0.16	0.17
17	-0.38	-0.55	0.63	-0.19	0.23	0.25

^a See ref 13. ^b A summary of structures 1-17 may be viewed in Figure 2.

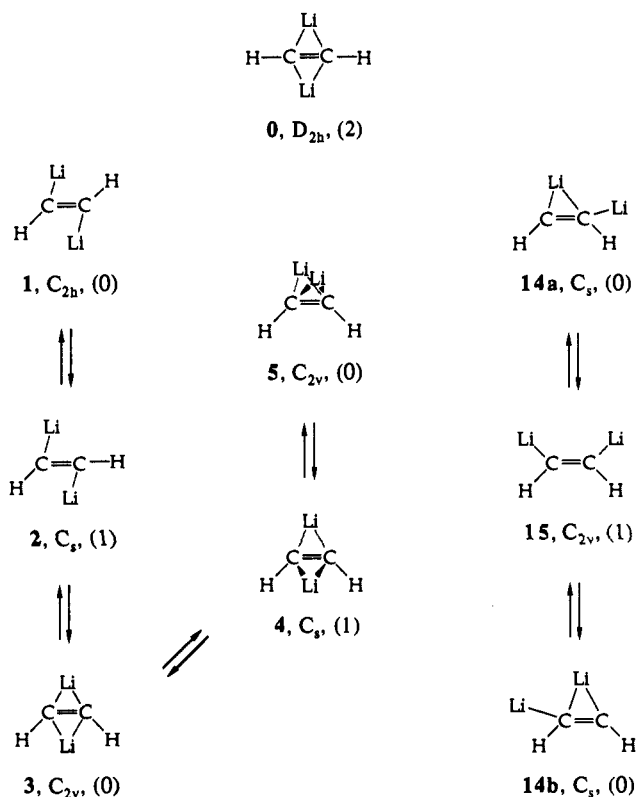


Figure 1. Previously studied (see refs 4 and 5) singlet 1,2-dilithioethene structures. For each structure, the symmetry and number of imaginary frequencies (in parentheses) are given.

retical investigation on the singlet 1,2-dilithioethene and acetylenic $C_2H_2Li_2$ potential energy surface attempts to answer questions raised by earlier work: What is the most stable 1,2-dilithioethene isomer with the hydrogens *cis* or *trans*? How do the relative energies of the lowest lying minima compare? What is the global $C_2H_2Li_2$ minimum?

Theoretical Methods

The first stage of this study surveyed the singlet dilithioethene potential energy surface (PES) to locate minima and symmetry-constrained transition states at lower levels of theory. The 1,2-dilithioethene minima, "acetylenic" $C_2H_2Li_2$ isomers, and the transition states that interconvert these various minima were then reexamined at higher theoretical levels. The Spartan 3.0¹¹ and Gaussian 92¹² program systems were used to search for stationary points at the restricted Hartree-Fock (RHF) level using STO-3G, 3-21G, and 6-31G** basis sets. NBO version 3.1,¹³ incorporated into Gaussian 92, was used for natural population analysis and computational of the natural charges. Complete geometry optimizations resulted in stationary points that were characterized by harmonic vibrational frequency (as well as IR intensity) computations. Next, additional complete surveys of the singlet PES employed MP2(FULL)/6-31G** (Møller-Plesset second-order perturbation theory) with all orbitals explicitly used in the correlation procedure.

Various methods were used to locate transition states for interconversion including mode following, linear synchronous transit, manual path following in constrained Cartesians, and standard^{12,14,15} methods.

(11) Spartan Version 3.0, Wavefunction, Inc., 18401 Von Karman, No. 370, Irvine, CA 92715. Copyright 1993 Wavefunction Inc.

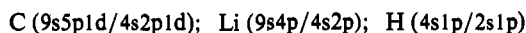
(12) Gaussian 92 Revision D2, Frisch, M. J.; Trucks, G. W.; Head-Gordon, M.; Gill, P. M. W.; Wong, M. W.; Foresman, J. B.; Johnson, B. G.; Schlegel, H. B.; Robb, M. A.; Replogle, E. S.; Gomperts, R.; Andres, J. L.; Raghavachari, K.; Binkley, J. S.; Gonzalez, C.; Martin, R. L.; Fox, D. J.; Defrees, D. J.; Baker, J.; Stewart, J. J. P.; Pople, J. A., Gaussian, Inc., Pittsburgh, PA, 1992. See also: Hehre, W. J.; Radom, L.; Pople, J. A.; Schleyer, P. v. R. *Ab Initio Molecular Orbital Theory*; John Wiley & Sons: New York, 1986. Foresman, J. B.; Frisch, A. *Exploring Chemistry with Electronic Structure Methods: A Guide to Using Gaussian*; Gaussian, Inc.: Pittsburgh, 1993.

(13) NBO Version 3.1, Glendening, E. D.; Reed, A. E.; Carpenter, J. E.; Weinhold, F. For a description, see: Reed, A. E.; Curtiss, L. A.; Weinhold, F. *Chem. Rev.* **1988**, *88*, 899-926.

(14) Pulay, P. In *Modern Theoretical Chemistry*; Schaefer, H. F., Ed.; Plenum Press: New York, 1977; Vol. 4.

Transition states connecting minima were verified by decent (in both directions) at the RHF/6-31G** and MP2/6-31G** levels.

As detailed in the following sections, seven minima and ten transition states were selected for further study using a different basis set, higher levels of theory, and the PSI 2.0.8 suite of programs.¹⁶ For carbon and hydrogen, the DZP basis is a standard Huzinaga-Dunning^{17,18} double- ζ basis set of contracted Gaussian functions augmented by a set of five Cartesian d-type polarization functions on carbon [$\alpha_d(C) = 0.75$] and a set of p-type polarization functions on hydrogen [$\alpha_p(H) = 0.75$]. The DZP basis set for lithium is a more flexibly contracted variant of the (9s4p/3s2p) set presented in Table A.1, Appendix 2, of the paper by Dunning and Hay.¹⁹ We uncontracted (i.e., assigned a contraction coefficient of 1.0 to) the primitive s functions with orbital exponents $\alpha = 0.444\ 62$ and $\alpha = 0.076\ 66$. The contraction scheme for our DZP basis is



The effects of electron correlation were assessed using configuration interaction including all single and double excitations from an RHF reference wave function (CISD), the coupled-cluster method including all single and double excitations (CCSD), and the CCSD method with connected triple excitations included perturbatively [CCSD(T)]. All orbitals were used in the electron correlation procedure.

All structures were optimized fully using closed-shell analytic gradient techniques at the RHF,^{14,20,21} CISD,²²⁻²⁴ and CCSD^{25,26} levels. In all cases, the residual Cartesian and internal coordinate gradients were less than 10^{-6} au. Harmonic vibrational frequencies were obtained using RHF analytic energy second-derivative techniques²⁷⁻²⁹ and central finite differences of analytic gradients for the CISD and CCSD methods.

Relative energies were also obtained by adding the Davidson correction³⁰ (designated CISD+Q) for unlinked quadruple excitations to the CISD energies. Improved estimates of the relative energy were determined using coupled-cluster methods with CCSD optimized geometries. The following notation is employed for these singlet-point energies: a CCSD-(T)/DZP energy³¹ evaluated with the CCSD/DZP optimized geometry is designated CCSD(T)/DZP//CCSD.

Results and Discussion

Previously reported singlet 1,2-dilithioethene stationary points are given in Figure 1 and relative energies in Table 1. The higher level results presented in this study agree with the previous characterization of minima and transition states^{4,5} at lower levels; however, the present study reveals that the earlier PES's were not exhaustively examined. Figure 2 shows 17 structures, 10 of which are new. Of these new structures, one is a *trans*-1,2-dilithioethene minima, 7. This planar, C_s symmetry form is reminiscent of 14,

(15) Fletcher, R. *Practical Methods of Optimization*; Wiley Press: New York, 1980; Vol. 1.

(16) PSI 2.0.8, Janssen, C. L.; Seidl, E. T.; Scuseria, G. E.; Hamilton, T. P.; Yamaguchi, Y.; Remington, R.; Xie, Y.; Vacek, G.; Sherill, C. D.; Crawford, T. D.; Fermann, J. T.; Allen, W. D.; Brooks, B. R.; Fitzgerald, G. B.; Fox, D. J.; Gaw, J. F.; Handy, N. C.; Laidig, W. D.; Lee, T. J.; Pitzer, R. M.; Rice, J. E.; Saxe, P.; Scheiner, A. C.; Schaefer, H. F., PSITECH, Inc., Watkinsville, GA, 1994.

(17) Huzinaga, S. *J. Chem. Phys.* **1965**, *42*, 1293-1302.

(18) Dunning, T. H. *J. Chem. Phys.* **1970**, *53*, 2823-2833.

(19) Dunning, T. H.; Hay, P. J. In *Modern Theoretical Chemistry*; Schaefer, H. F., Ed.; Plenum Press: New York, 1977; Vol. 3.

(20) Dupuis, M.; King, H. F. *J. Chem. Phys.* **1978**, *68*, 3998-4004.

(21) Goddard, J. D.; Handy, N. C.; Schaefer, H. F. *J. Chem. Phys.* **1979**, *71*, 1525-1530.

(22) Osamura, Y.; Yamaguchi, Y.; Schaefer, H. F. *J. Chem. Phys.* **1982**, *77*, 383-390.

(23) Brooks, B. R.; Laidig, W. D.; Saxe, P.; Goddard, J. D.; Yamaguchi, Y.; Schaefer, H. F. *J. Chem. Phys.* **1980**, *72*, 4652-4653.

(24) Rice, J. E.; Amos, R. D.; Handy, N. C.; Lee, T. J.; Schaefer, H. F. *J. Chem. Phys.* **1986**, *85*, 963-968.

(25) Scheiner, A. C.; Scuseria, G. E.; Rice, J. E.; Lee, T. J.; Schaefer, H. F. *J. Chem. Phys.* **1987**, *87*, 5361-5373.

(26) Purvis, G. D.; Bartlett, R. J. *J. Chem. Phys.* **1982**, *76*, 1910-1918.

(27) Pople, J. A.; Krishnan, R.; Schlegel, H. B.; Binkley, J. S. *Int. J. Quantum Chem.* **1975**, *S13*, 225-241.

(28) Saxe, P.; Goddard, J. D.; Yamaguchi, Y.; Schaefer, H. F. *J. Chem. Phys.* **1982**, *77*, 5647-5654.

(29) Osamura, Y.; Yamaguchi, Y.; Saxe, P.; Fox, D. J.; Vincent, M. A.; Schaefer, H. F. *J. Mol. Struct.* **1983**, *103*, 183-196.

(30) Langhoff, S. R.; Davidson, E. R. *Int. J. Quantum Chem.* **1974**, *8*, 61-72.

(31) Scuseria, G. E.; Lee, T. J. *J. Chem. Phys.* **1990**, *93*, 5851-5856.

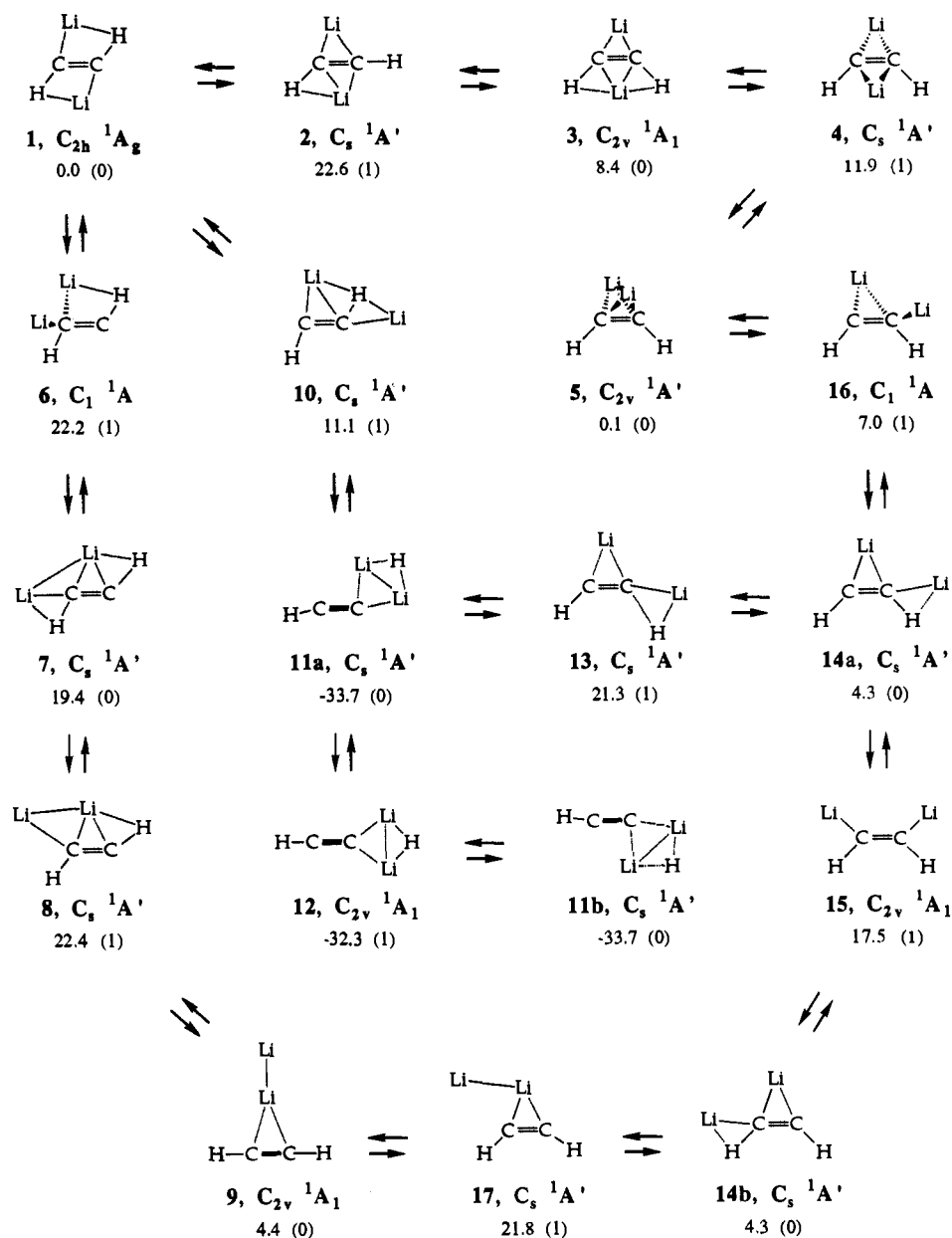


Figure 2. Singlet 1,2-dilithioethene PES as determined in the present research. For each structure, the symmetry, electronic state, CCSD/DZP (+ZPVE) corrected relative energy (kcal/mol), and number of imaginary frequencies (in parentheses) are given.

a planar, C_s symmetry *cis*-1,2-dilithioethene, monobridged lithium structure. A C_1 symmetry transition state, 6, provides a 7 → 1 path corresponding to an out-of-plane bending motion of the nonbridged lithium in 7 over the C—H bond and across the C=C bond.

Figure 2 also contains two previously unreported singlet $C_2H_2Li_2$ minima, 9 and 11, which possess “acetylenic” character. Structure 9 is a planar, C_{2v} symmetry complex of acetylene and Li_2 . The lithium dimer is oriented along the C_2 axis, perpendicular to the C≡C triple bond. The other stable “acetylenic” form of $C_2H_2Li_2$, 11, is a planar, C_s symmetry state that can be visualized electrostatically as a complex of the acetylene anion, $HC\equiv C^-$, with Li_2H^+ . A planar C_{2v} symmetry transition state, 12, provides a path for interconversion of 11a into its degenerate mirror image, 11b, through an in-plane bending motion of the hydride ion.

Paths from the singlet 1,2-dilithioethene PES surface to the singlet acetylenic structures were considered. The transition state for the 7 → 9 path, 8, corresponds to a symmetric CCH bending mode and involves breaking the interaction between the nonbridged lithium and one of the carbon atoms. The transition state for 14 → 9, 17, occurs in a similar fashion, but the hydrogens are *cis* as opposed to *trans* in 8.

Two paths from the singlet 1,2-dilithioethene PES were found

leading to structure 11. The transition state, 10, for the 1 → 11 conversion portrays the breaking of a C—H bond in 1 stabilized by interactions with two lithium ions positioned on each side of the leaving hydrogen. Structure 13, the transition structure in the 14 → 11 pathway, is similar to that in 1 → 11, in that it involves the breaking of a C—H bond. However, unlike 10, only one lithium helps the removal of the hydrogen and its transformation into a hydride ion.

A low-lying pathway between between the previously reported *cis*-1,2-dilithioethene minima (14 → 5) also has been found. The *cis* transition structure, 16, is very similar to *trans* 6 in the 1 → 7 pathway. The 14 → 5 pathway corresponds to an out-of-plane bending mode of the nonbridged lithium in 16.

Molecular fragments LiH , $HC\equiv CLi$, Li_2 , and $HC\equiv CH$ are computed individually at the same levels of theory [Tables 2–5] for energetic and structural comparisons. Natural population analysis¹³ is performed on each structure considered in this study, and the computed natural charges are summarized in Table 6. The results for structures 1–17 are given in Tables A–Q (supplementary material) and Figures 3–19, respectively.

An arbitrary convention for drawing structures has been employed due to the large variation in the C—Li, Li—Li, and Li—H distances. All C—Li distances under 2.0 Å, Li—Li distances less

Table 7. Energetic Comparison (Relative Energies (kcal/mol)) of All Stationary Points Characterized on the Singlet 1,2-Dilithioethene PES

structure ^a	level of theory						
	RHF/6-31G**	MP2/6-31G**	RHF/DZP	CISD/DZP	CISD+Q/DZP ^b	CCSD/DZP	CCSD(T)/DZP//CCSD ^c
1	0.0	0.0	0.0	0.0	0.0	0.0	0.0
2	26.1	23.0	26.1	24.7	22.6	24.2	23.7
3	11.1	9.9	10.9	9.5	9.0	9.0	8.6
4	14.2	14.5	14.2	13.8	13.5	13.5	13.4
5	2.1	2.0	1.6	0.6	-0.1	-0.3	-0.8
6	27.7	27.4	26.0	25.2	24.4	23.5	22.3
7	27.7	22.6	25.0	23.8	22.6	20.7	16.0
8	35.9	24.6	34.2	29.9	26.0	24.2	20.4
9	2.1	11.3	1.5	9.5	8.9	5.4	6.3
10	14.0	18.4	12.6	14.5	14.2	14.4	14.1
11	-35.8	-29.5	-36.5	-31.3	-30.7	-30.4	-30.1
12	-33.5	-26.7	-35.1	-29.7	-29.1	-28.8	-28.5
13	26.2	27.5	25.9	27.0	25.7	25.6	24.1
14	6.4	7.6	4.2	5.3	5.2	5.0	4.9
15	20.5	23.4	19.0	19.9	19.5	18.9	18.4
16	8.3	10.2	7.4	8.1	7.9	7.6	7.4
17	28.7	25.7	27.7	28.3	25.8	23.8	21.2
Li ₂ + HCCH	7.4	19.6	5.1	14.6	14.2	10.8	12.1
LiH + LiCCH	15.8	24.9	12.3	19.3	19.9	19.8	20.3

^a Summary of the structures may be viewed in Figure 2. ^b All relative energies in this column correspond to a comparison of the Davidson correction energies at the CISD/DZP optimized geometries. ^c All relative energies in this column correspond to a comparison of the single point CCSD(T)/DZP energies at CCSD/DZP optimized geometries.

Table 8. Energetic Comparison (Relative Energies (kcal/mol)) of Stationary Points Examined on the Singlet 1,2-Dilithioethene PES^a

structure ^b	level of theory						
	RHF/6-31G**	MP2/6-31G**	RHF/DZP	CISD/DZP	CISD+Q/DZP ^c	CCSD/DZP	CCSD(T)/DZP//CCSD ^d
1	0.0	0.0	0.0	0.0	0.0	0.0	0.0
2	24.7	21.3	24.6	23.1	21.0	22.6	22.2
3	10.6	9.0	10.4	8.9	8.4	8.4	7.9
4	12.8	12.8	12.8	12.2	11.9	11.9	11.8
5	2.4	2.0	2.0	0.9	0.3	0.1	-0.4
6	26.6	26.2	24.8	24.1	23.3	22.2	20.9
7	26.7	21.9	24.1	22.8	21.6	19.4	14.8
8	34.4	22.8	32.6	28.3	24.4	22.4	18.6
9	1.8	9.8	1.0	8.6	8.0	4.4	5.2
10	10.7	15.0	9.4	11.0	10.7	11.1	10.8
11	-39.1	-33.1	-39.7	-34.7	-34.1	-33.7	-33.5
12	-36.9	-30.6	-38.4	-33.2	-32.6	-32.3	-32.0
13	21.8	23.2	21.4	22.6	21.3	21.3	19.9
14	6.0	7.0	3.9	4.8	4.7	4.3	4.2
15	19.4	21.8	17.9	18.6	18.2	17.5	17.0
16	7.8	9.4	7.1	7.5	7.3	7.0	6.9
17	27.1	23.7	26.0	26.5	24.0	21.8	19.2
Li ₂ + HCCH	4.0	15.4	1.6	10.8	10.4	7.0	8.2
LiH + LiCCH	8.6	17.5	5.1	12.0	12.6	12.7	13.2

^a Zero point vibrational energy (ZPVE) corrections (kcal/mol) are included in the relative energies presented here. ^b A summary of the structures may be viewed in Figure 2. ^c All relative energies in this column correspond to a comparison of the Davidson correction energies at CISD/DZP optimized geometries using the CISD/DZP ZPVE correction. ^d All relative energies in this column correspond to a comparison of the single point CCSD(T)/DZP energies at CCSD/DZP optimized geometries using the CCSD/DZP ZPVE correction.

than 2.8 Å, and Li-H distances less than 1.7 Å are shown as white lines outlined in black. All C-Li distances between 2.0 and 2.15 Å, Li-Li distances between 2.8 and 3.0 Å, and Li-H distances between 1.7 and 1.95 Å are shown as solid black lines. Figures 3-19 reflect these conventions and also include a depiction of the canonical HOMO superimposed on an electrostatic interpretation.

Bonding Considerations. Structure 1, summarized in Figure 3 and Table A (supplementary material), is a planar, C_{2h} symmetry minimum with acute Li-C-C bond angles. ACKJS⁴ reasoned that these acute Li-C-C bond angles were partially due to σ and π electronic interactions. More recent interpretations have emphasized the ionic interactions.⁵ A smaller C-C-Li angle reduces the C_{β} -Li distances and gives rise to better electrostatic bonding. The large natural charges for carbon and lithium, -0.92 and +0.82, respectively, support an ionic interpretation for the bonding of the *trans* vinyl dianion with two lithium cations.

Structure 3 for *cis*-1,2-dilithioethene [Figure 5 and Table C (supplementary material)] has C_{2v} symmetry with planar tetracoordinate carbons and dibridged lithiums. Examination of the canonical occupied molecular orbitals reveals π overlap

between the C=C double bond and empty Li 2p orbitals in the HOMO-1. The C-Li(3) distances are 0.013 Å shorter at CISD/DZP than the C-Li(4) distances. The shorter C-Li(3) distance allows better electrostatics as well as better π overlap with the carbon lone pairs which overcome the Li-H electrostatic repulsion. The natural population analysis supports a picture of electrostatic interaction between the *cis* vinyl dianion and two Li⁺ ions. While ionic interactions predominate, we find evidence for the contribution of some π bonding.

A previously reported minimum, 5 [Figure 7 and Table E (supplementary material)], is the nonplanar, C_{2v} symmetry *cis*-1,2-dilithioethene structure with dibridged lithiums. The Li-Li distance, 2.628 Å at CISD/DZP, is shorter than the value computed for the isolated lithium dimer, 2.733 Å at the same level of theory. As shown in Figure 7, 5 appears to have a Li₂ moiety perpendicular to the C=C double bond. This is deceiving, however. The Weinhold natural charges on carbon (-0.94) and lithium (+0.75) result in strong electrostatic interactions between the *cis* vinyl dianion and the two Li⁺ cations. This is similar to the situation in 3, except that the preferred Li⁺ orientations in

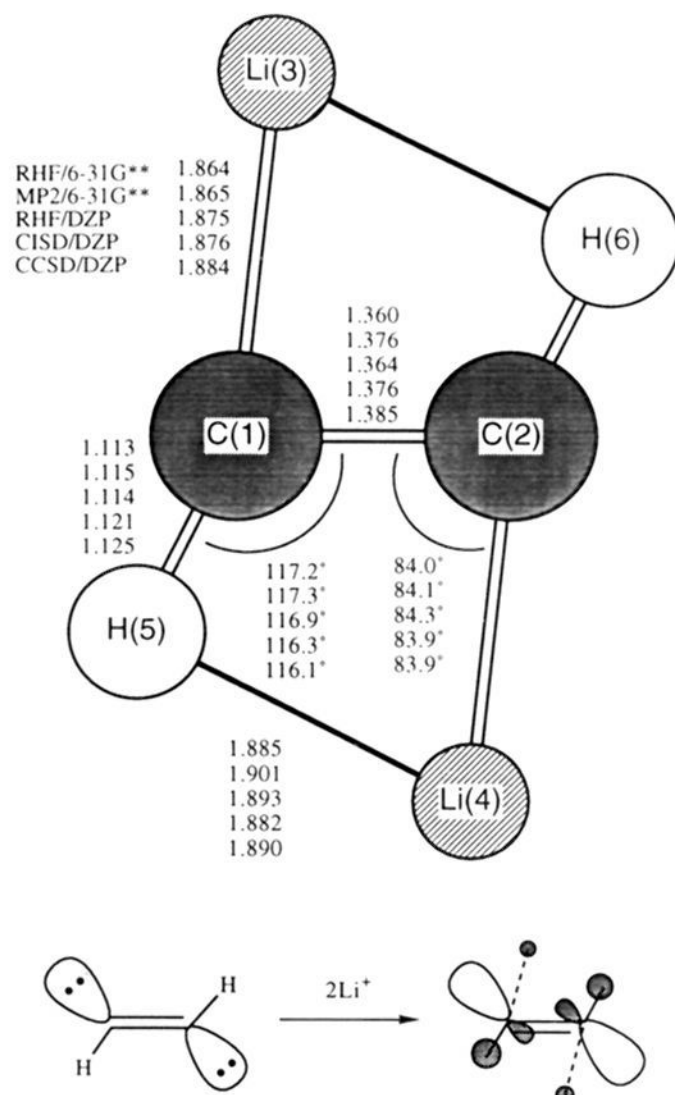


Figure 3. Summary of theoretical equilibrium geometries for structure **1**, the planar 1A_g state of the *trans*-1,2-dilithioethene molecule, and an electrostatic interpretation with a qualitative representation of the canonical HOMO superimposed. Bond distances are in angstroms, and bond angles are in degrees.

5 are perpendicular to the HCCH plane. This orientation stresses the ion quadrupole nature of **5**. No Li—Li bonding is involved.³²

A planar, C_s *trans*-1,2-dilithioethene structure, **7** [Figure 9 and Table G (supplementary material)], is quite different. Both lithiums in **7** appear to be bound preferentially to one carbon, based on the C—Li distances. The natural charges are not as large as those found with other structures. The natural charges calculated for structures **1**, **3**, and **5** (Table 6) were consistently greater than -0.90 for carbon and $+0.74$ for lithium. The carbon and lithium charges on **7** are -0.69 , -0.41 , $+0.13$, and $+0.61$ for C(1), C(2), Li(3), and Li(4), respectively. This is not surprising, however, and can be understood by examining the charges on Li₄ in structure **1** as it progresses toward **9** and the formation of an Li—Li bond. The path **1** ($+0.82$) \rightarrow **6** ($+0.67$) \rightarrow **7** ($+0.13$) \rightarrow **8** (-0.08) \rightarrow **9** (-0.18) shows the lithium charges (in parentheses) becoming increasingly negative as the Li—Li bond forms. Large changes in the C—Li and Li—Li distances and dramatic variation of the dipole moment at the MP2/6-31G** and CCSD/DZP levels, however, indicate there is some disagreement with respect to the level of theory as to the extent of Li—Li interaction in **7**.

Structure **9** [Figure 11 and Table I (supplementary material)] is essentially a van der Waals complex of dilithium interacting with acetylene, with large C—Li separations (2.552 \AA at CCSD/DZP). The canonical HOMO does not suggest bonding between Li₂ and acetylene and depicts only π bonding between the carbon atoms. The third highest canonical occupied molecular orbital (HOMO-3), however, shows a diffuse Li—Li covalent σ bond interacting with acetylene. Polarization of Li₂ results in a slight positive charge on Li(3) and a counterbalancing negative charge on Li(4).

The canonical HOMO sketches for the transition states leading to **9**, **8** (Figure 10) and **17** (Figure 19), are different than

(32) Supported by examination of the total electron density, canonical molecular orbitals, and natural bonding analysis.

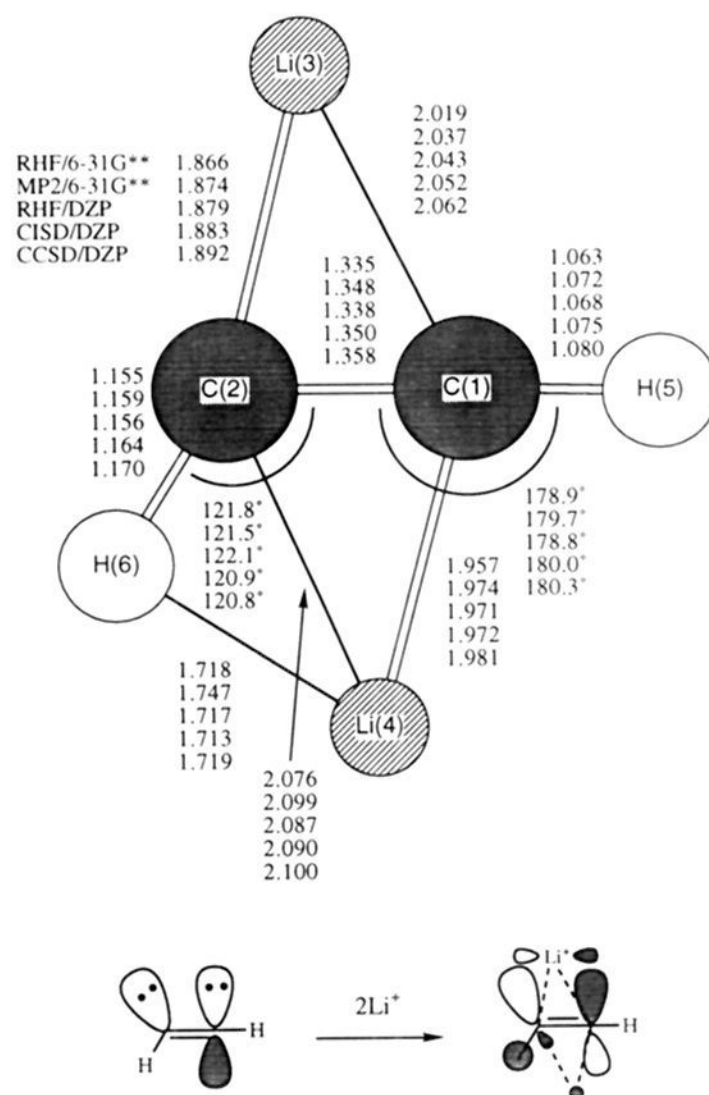


Figure 4. Summary of theoretical geometries for structure **2**, the planar $^1A'$ transition state of the 1,2-dilithioethene molecule that interconverts structures **1** and **3**, and an electrostatic interpretation with a qualitative representation of the canonical HOMO superimposed. Bond distances are in angstroms, and bond angles are in degrees.

for the other structures. The nonbridged lithium in these sketches is depicted as having a diffuse " σ -like" orbital. Since the transition states involve the breaking or formation of a diffuse Li—Li bond, this is not surprising. The natural charges on the nonbridged lithiums, -0.08 (**8**) and -0.19 (**17**), are close to the values obtained for the nonbridged lithium in **9**, -0.18 , implying the nonbridged lithiums retain an appreciable quantity of electron density much unlike other structures where the lithium atoms are significantly ionic. Therefore, it is not unexpected that the nonbridged lithiums in **8** and **17** should exhibit σ -like character in their respective HOMO.

The acetylenic¹¹ **11** [Figure 13 and Table K (supplementary material)] has a very short Li—Li distance, 2.451 \AA at CISD/DZP, but no Li—Li bonding interactions are indicated.³² The electrostatic depiction of **11** as a stable ionic complex between $HC\equiv C^-$ and $LiHLi^+$ is supported by the computed natural charges. The stability is enhanced by the ion quadrupole character since both lithiums possess large positive charges, and C(2) and H(5) provide the counterbalancing negative charges. This acetylenic¹¹ structure is related to the stable complex proposed by MGD⁹ from the experimental observations.

Structures **10** (Figure 12) and **13** (Figure 15), the transition states leading to the complex **11** from the *trans* and *cis* portions of the singlet 1,2-dilithioethene PES, respectively, involve the abstraction of a hydrogen atom from the C_2H_2 unit. As Table 6 shows this hydrogen atom possesses hydride character with a negative natural charge, -0.41 and -0.49 , for both **10** and **13**, respectively. Large positive charges on the lithium atoms relative to the negatively charged hydrogen atom also help explain the large dipole moments for both **10** and **13**, 5.96 and 7.87 D at CCSD/DZP, respectively.

The previously reported planar, C_s *cis*-1,2-dilithioethene minimum, **14** [Figure 16 and Table M (supplementary material)], has a monobridged lithium and resembles the *cis* analog of **7**. However, the atomic charges in **14** are not like those in **7**. The

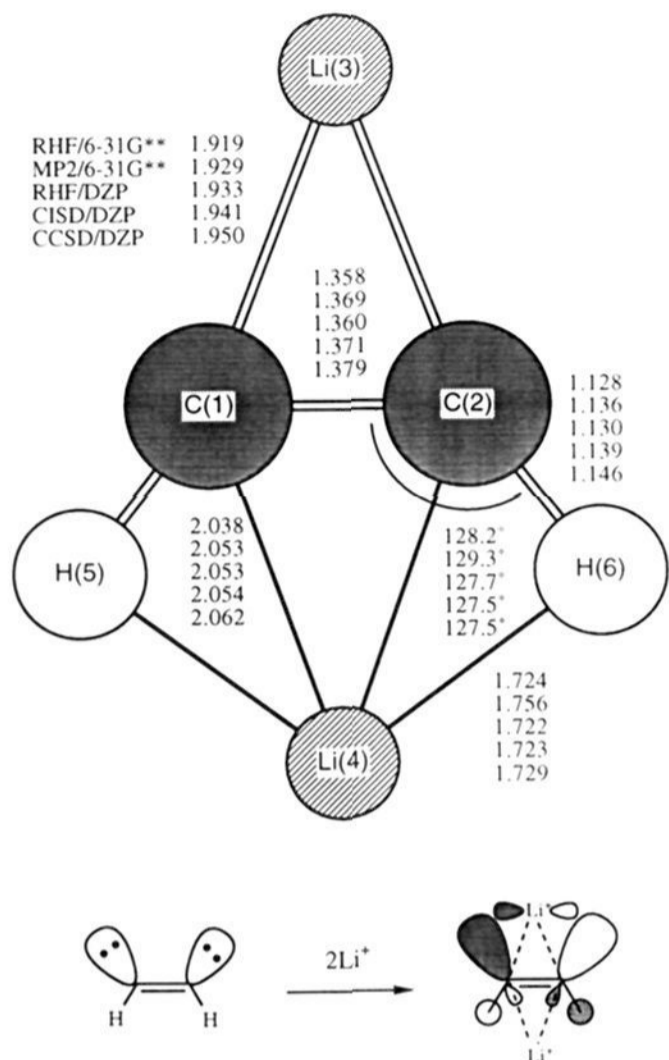


Figure 5. Summary of theoretical equilibrium geometries for structure **3**, the planar dibridged 1A_1 state of the *cis*-1,2-dilithioethene molecule, and an electrostatic interpretation with a qualitative representation of the canonical HOMO superimposed. Bond distances are in angstroms, and bond angles are in degrees.

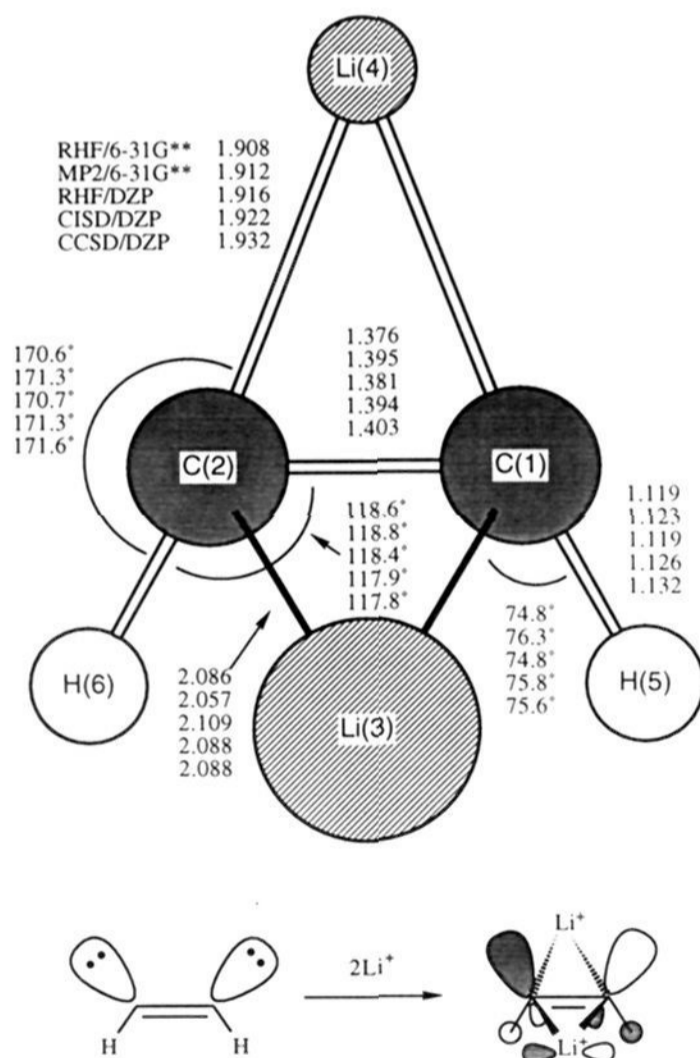


Figure 6. Summary of theoretical geometries for structure **4**, the dibridged 1A_1 transition state of the *cis*-1,2-dilithioethene molecule that interconverts structures **3** and **5**, and an electrostatic interpretation with a qualitative representation of the canonical HOMO superimposed. Bond distances are in angstroms, and bond angles are in degrees.

canonical HOMO-1 delineates π overlap between the C=C double bond and the monobridged Li(3). From an electrostatic

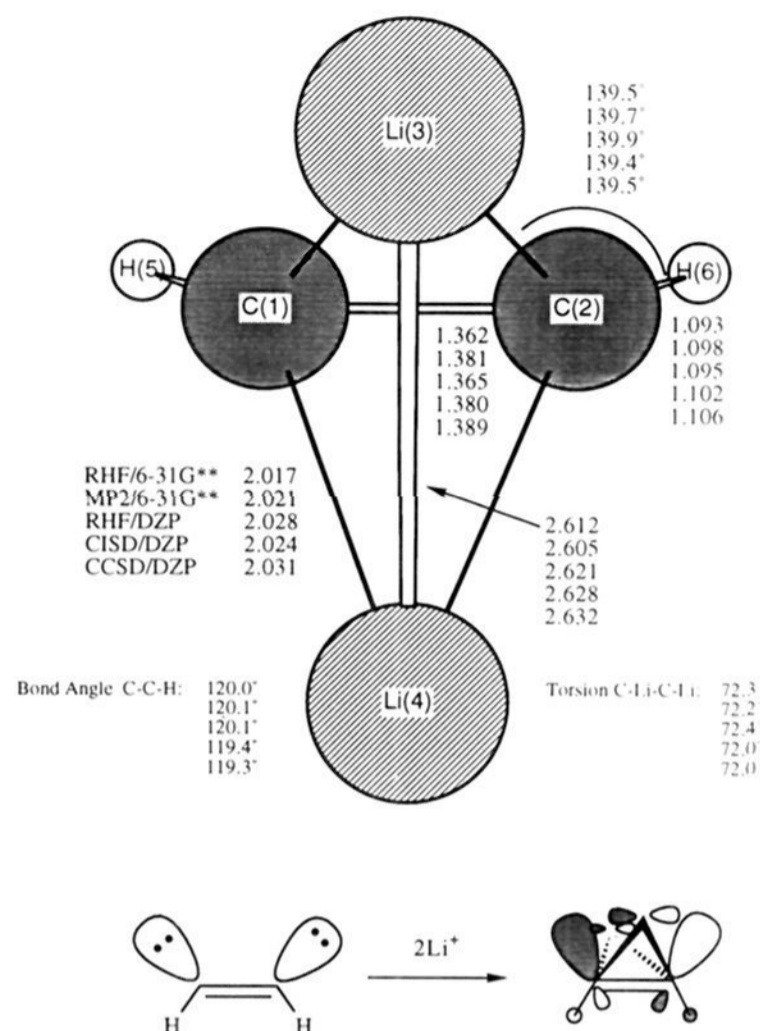


Figure 7. Summary of theoretical equilibrium geometries for structure **5**, the twisted dibridged 1A_1 state of the *cis*-1,2-dilithioethene molecule, and an electrostatic interpretation with a qualitative representation of the canonical HOMO superimposed. Bond distances are in angstroms, and bond angles are in degrees. For clarity, in this sketch only the Li designations are deleted.

point of view, Li(3) nestles between two lone pairs and Li(4) interacts with a lone pair and an electron-rich C—H bond. Both configurations of Li^+ ions are highly favorable. The position of the Li^+ ions relative to the lone pairs results in the large dipole moment, 7.73 D at CCSD/DZP.

Energetic Comparisons. Table R (supplementary material) summarizes the total energies with the Davidson corrections, designated as CISD+Q/DZP, and the CCSD(T)/DZP single points at CCSD/DZP optimized geometries, CCSD(T)/DZP //CCSD, for all structures and molecular fragments, examined in this study. Relative energies without and with ZPVE corrections are given in Tables 7 and 8, respectively.

The global minimum of the $\text{C}_2\text{H}_2\text{Li}_2$ PES clearly³³ is structure **11**, the C_s complex between $\text{HC}\equiv\text{CLi}$ and LiH . It lies 33.7 kcal/mol below the lowest lying singlet 1,2-dilithioethene structure at CCSD/DZP with ZPVE correction [(+ZPVE)]. A relatively small barrier, 1.4 kcal/mol at CCSD/DZP (+ZPVE), interconverts **11a** with its degenerate mirror image, **11b**. Energetic comparison of the complex **11** with the separated species, $\text{HC}\equiv\text{CLi}$ and LiH , shows **11** is stable toward elimination of LiH , being 46.4 kcal/mol lower lying than the separated species at CCSD/DZP (+ZPVE).

The most stable *trans* minimum (**1**), the C_{2h} form with acute CCLi angles, is converted into the global minimum (**11**) via **10** (Figure 2). Thus, the elimination of HLi does not occur, and the barrier for the reorganization, **1** \rightarrow **11**, requires 11 kcal/mol.

More than one pathway is possible for the conversion of the most stable *cis* isomer (the doubly bridged C_{2v} structure **5**) into **11**. The highest barrier (represented by **2**) along the **5** \rightarrow **4** \rightarrow **3** \rightarrow **2** \rightarrow **1** \rightarrow **10** \rightarrow **11** pathway requires 22.6 kcal/mol. A similar barrier, 21.2 kcal/mol (for **13**), is found for the second pathway (**5** \rightarrow **16** \rightarrow **14a** \rightarrow **13** \rightarrow **11**).

(33) Bolton, E. E.; Laidig, W. D. Unpublished PES studies of the triplet 1,2-dilithioethene, triplet and singlet 1,1-dilithioethene, and acetylenic $\text{C}_2\text{H}_2\text{-Li}_2$ PES.

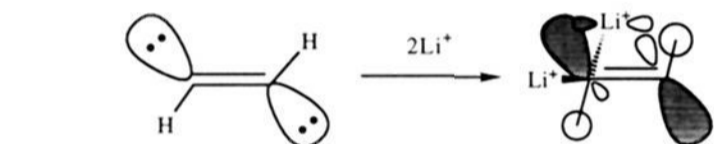
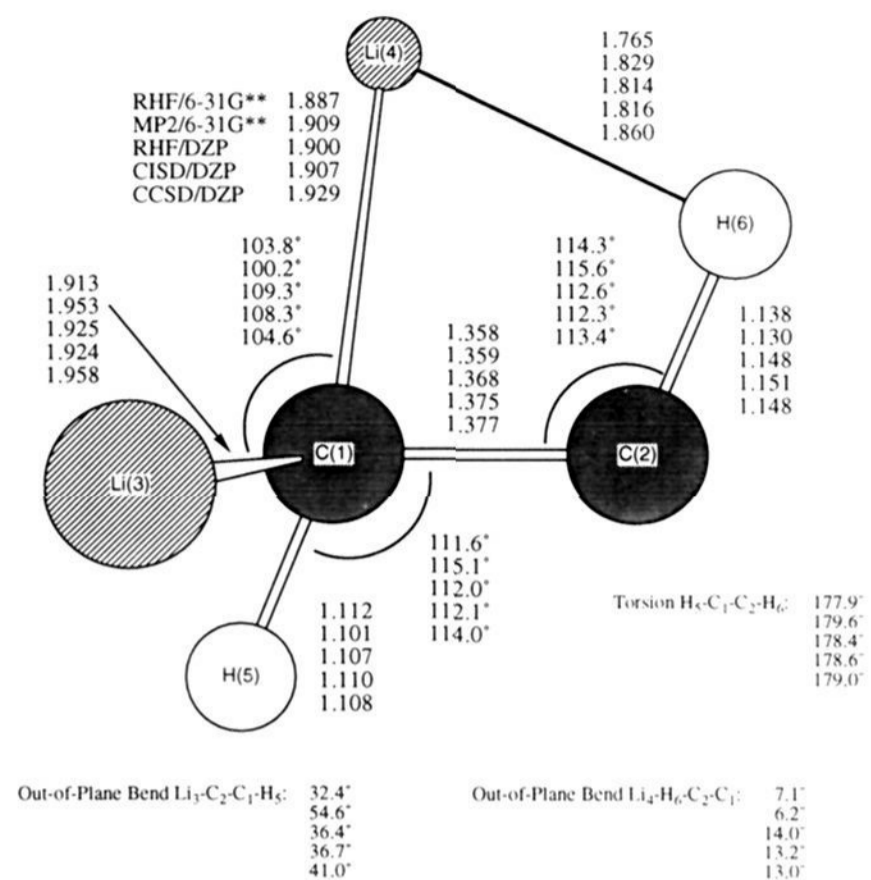


Figure 8. Summary of theoretical geometries for structure 6, the 1A transition state of the *trans*-1,2-dilithioethene molecule that interconverts structures 1 and 7, and an electrostatic interpretation with a qualitative representation of the canonical HOMO superimposed. Bond distances are in angstroms, and bond angles are in degrees.

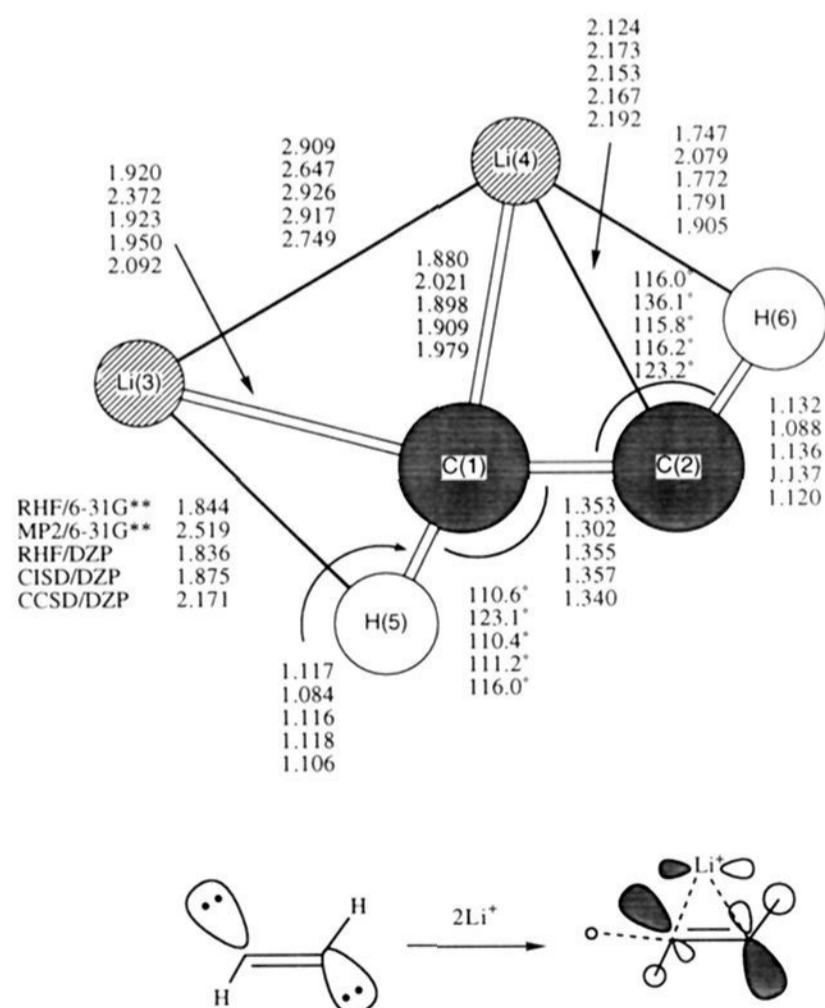


Figure 9. Summary of theoretical equilibrium geometries for structure 7, the planar 1A state of the *trans*-1,2-dilithioethene molecule, and an electrostatic representation with a qualitative representation of the canonical HOMO superimposed. Bond distances are in angstroms, and bond angles are in degrees.

The barrier for *cis* structures to rearrange to the global minimum is significantly higher than for *trans* structures. A 5

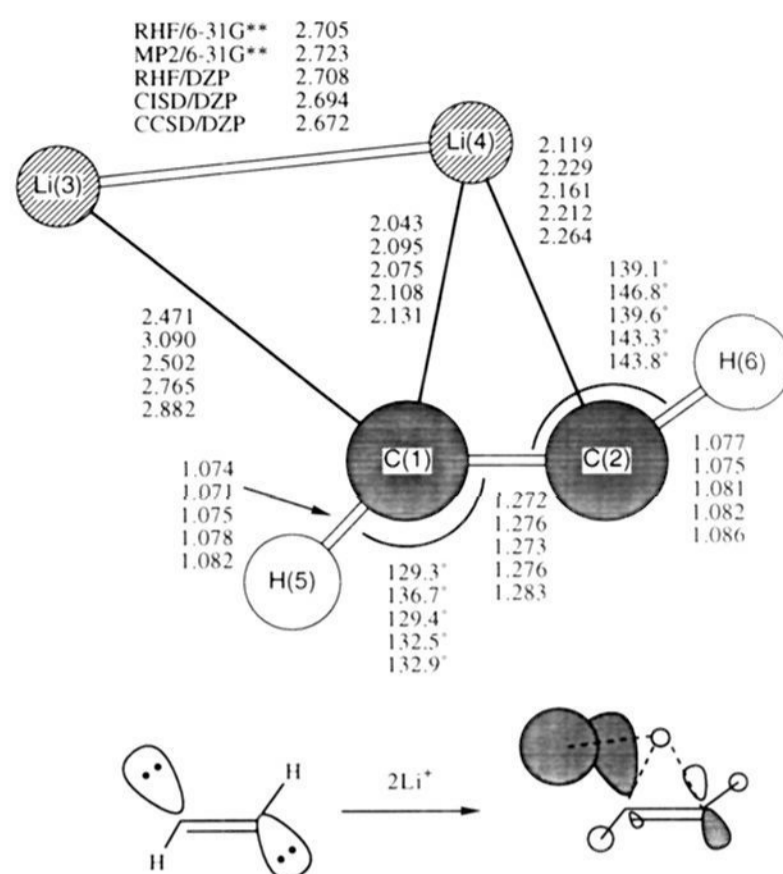


Figure 10. Summary of theoretical geometries for structure 8, the planar $^1A'$ transition state that interconverts structures 7 and 9, and an electrostatic representation with a qualitative representation of the canonical HOMO superimposed. Bond distances are in angstroms, and bond angles are in degrees. See the text for explanation of why the Li(3) atom in the sketch looks different from that in the sketches for the other structures.

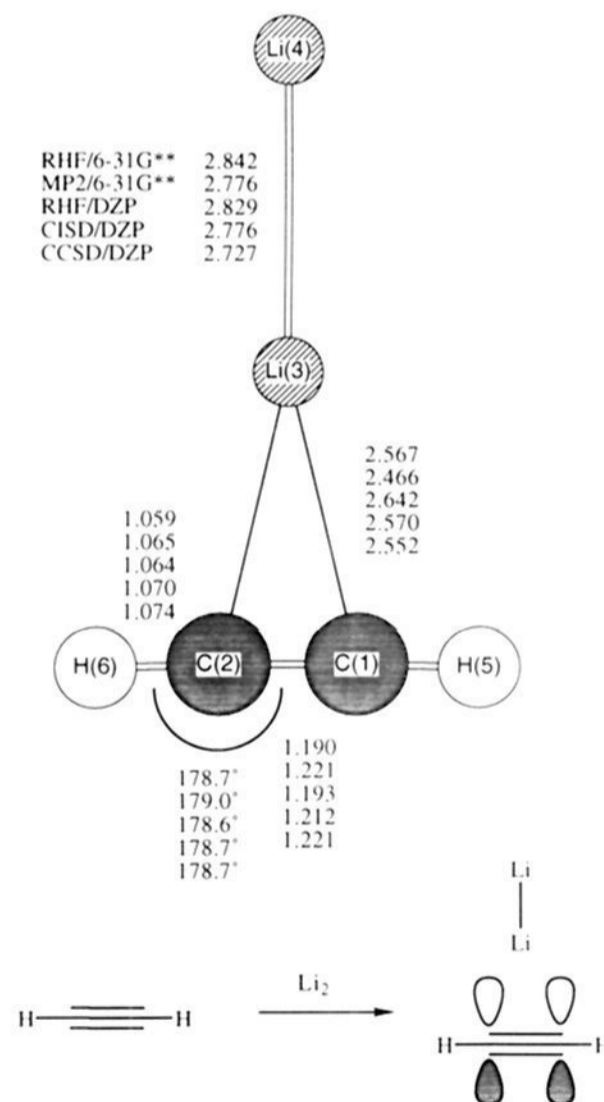


Figure 11. Summary of theoretical equilibrium geometries for structure 9, the planar 1A_1 state of the acetylene-lithium dimer complex, and an electrostatic interpretation with a qualitative representation of the canonical HOMO superimposed. Bond distances are in angstroms, and bond angles are in degrees.

\rightarrow 11 rearrangement has a barrier about twice that for 1 \rightarrow 11 rearrangement.

Two pathways exist for the addition of Li_2 to acetylene. One path (via 9 \rightarrow 8 \rightarrow 7 \rightarrow 6 \rightarrow 1) leads to the most stable *trans*

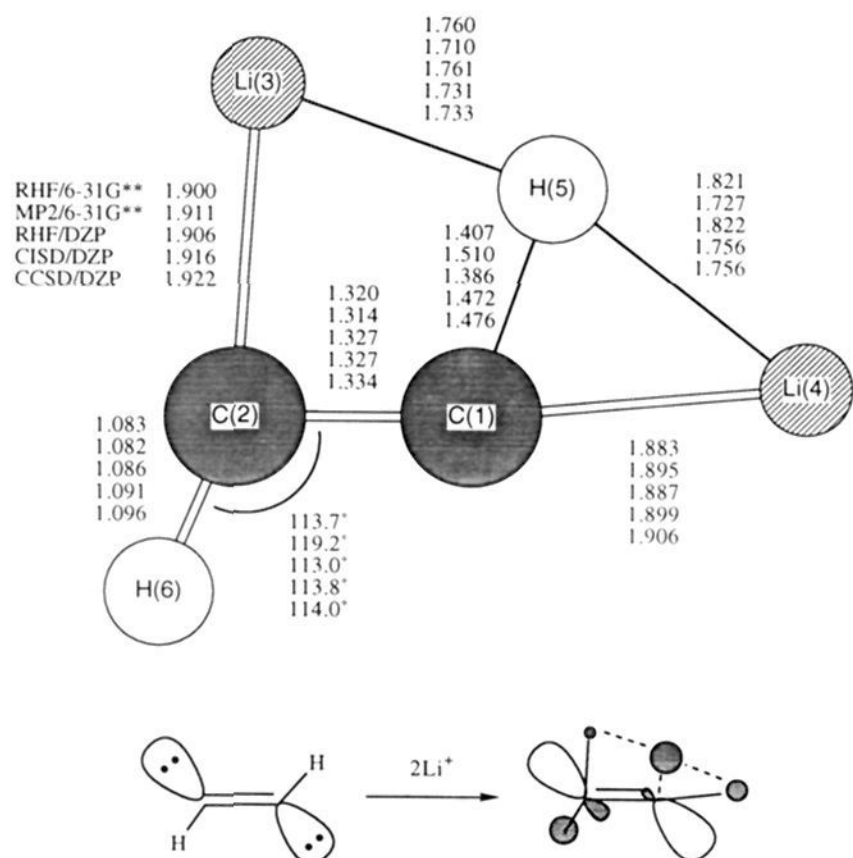


Figure 12. Summary of theoretical geometries for structure **10**, the planar $^1A'$ transition state that interconverts structures **1** and **11**, and an electrostatic interpretation with a qualitative representation of the canonical HOMO superimposed. Bond distances are in angstroms, and bond angles are in degrees.

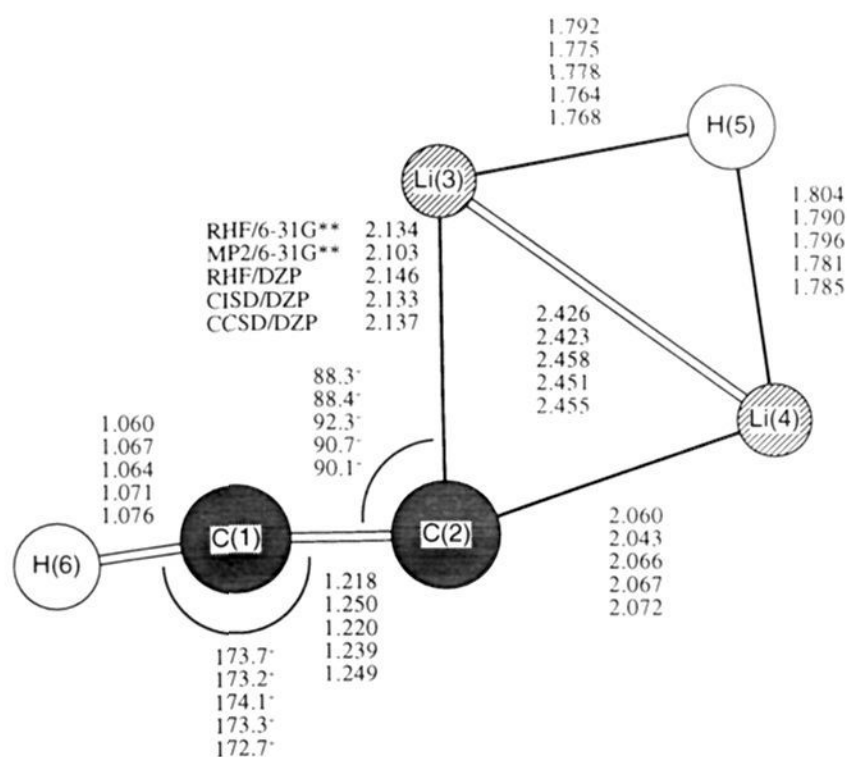


Figure 13. Summary of theoretical equilibrium geometries for structure **11**, the planar $^1A'$ state of the $C_2H_2Li_2$ complex and an electrostatic representation with a qualitative representation of the canonical HOMO superimposed. Bond distances are in angstroms, and bond angles are in degrees. This structure appears to be the global minimum for $C_2H_2Li_2$.

form **1** with a barrier of 18.0 kcal/mol, for **8**, while the other (via **9** \rightarrow **17** \rightarrow **14** \rightarrow **16** \rightarrow **5**) leads to the most stable *cis* form **5** and a comparable barrier of 17.4 kcal/mol, represented by **17**.

The most stable singlet 1,2-dilithioethene minimum is *trans* **1**, at all fully geometry optimized levels of theory and when ZPVE corrections are taken into consideration. A *cis* singlet 1,2-dilithioethene structure, **5**, however, is within 0.1 kcal/mol of **1** at CCSD/DZP (+ZPVE), the highest level of optimization, and is -0.3 kcal/mol lower in energy at CCSD/DZP. The CCSD-

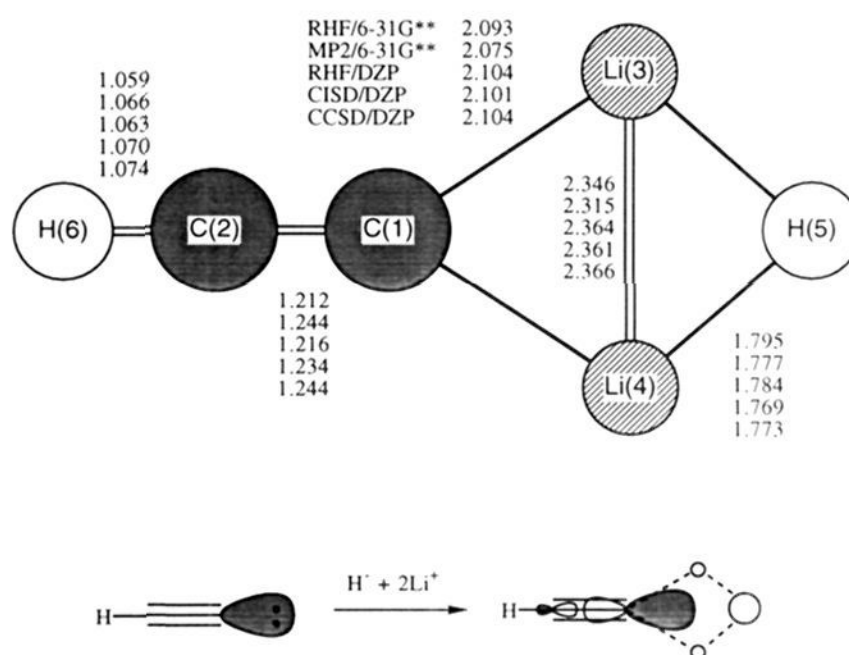


Figure 14. Summary of theoretical geometries for structure **12**, the planar 1A_1 transition state of the $C_2H_2Li_2$ complex that interconverts structure **11a** into its mirror image **11b**, and an electrostatic interpretation with a qualitative representation of the canonical HOMO superimposed. Bond distances are in angstroms, and bond angles are in degrees.

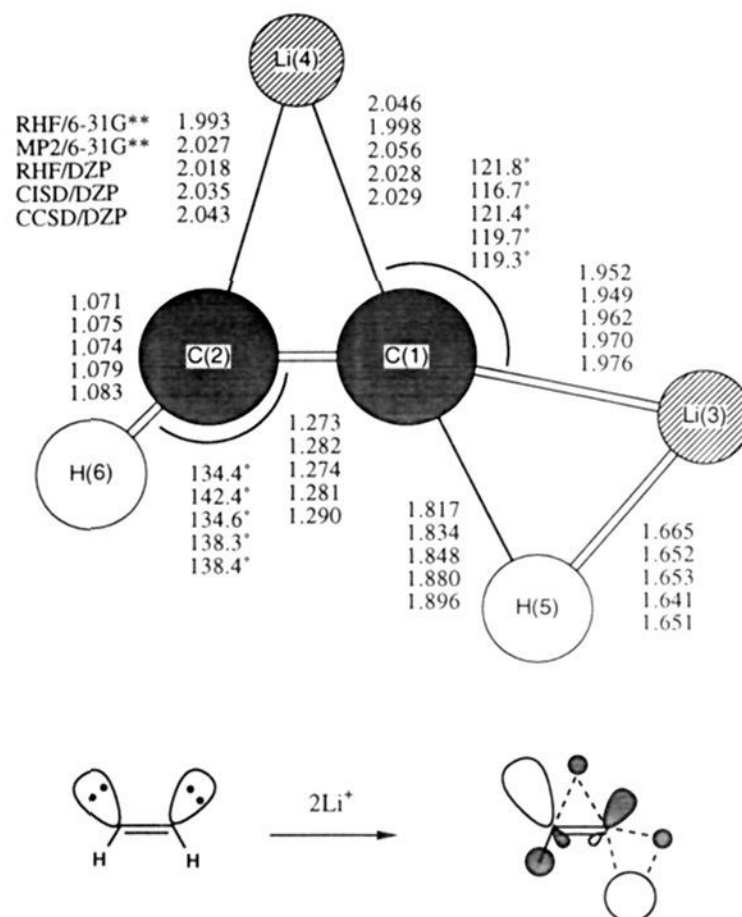


Figure 15. Summary of theoretical geometries for structure **13**, the planar $^1A'$ transition state that interconverts structures **14** and **11**, and an electrostatic interpretation with a qualitative representation of the canonical HOMO superimposed. Bond distances are in angstroms, and bond angles are in degrees.

(T)/DZP//CCSD level, with and without CCSD/DZP ZPVE corrections, predicts **5** will be lower in energy than **1** by 0.8 and 0.4 kcal/mol, respectively. The differences in energy between **1** and **5** are within 3 kcal/mol at all levels of theory applied.

The energies relative to **1** of the remaining singlet 1,2-dilithioethene minima considered are 8.4 (**3**), 19.4 (**7**), 4.4 (**9**), and 4.3 (**14**) kcal/mol at the CCSD/DZP (+ZPVE) level.

The effects of electron correlation are most pronounced for **7**. Increasing levels of correlation decrease its relative energy by 10.9 kcal/mol from RHF/6-31G** to CCSD(T)/DZP//CCSD. Analysis of the T_1 diagnostic,³⁴ the Euclidean norm of the t_1 vector of the coupled-cluster wave function, helps give insight to this significant increase in stability with respect to the level of

(34) The T_1 diagnostic is the Euclidean norm of the t_1 vector in the CCSD wave function and a useful measure of the orbital relaxation. See also refs 35 and 36 and references therein.

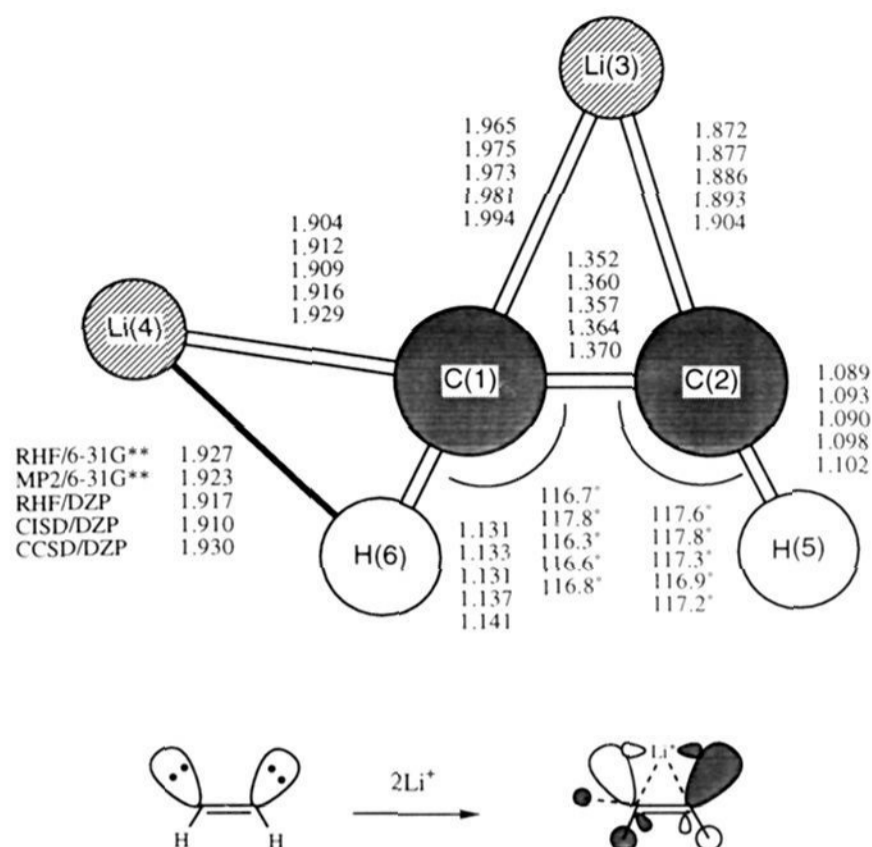


Figure 16. Summary of theoretical equilibrium geometries for structure **14**, the planar monobridged $^1A'$ state of the *cis*-1,2-dilithioethene molecule, and an electrostatic interpretation with a qualitative representation of the canonical HOMO superimposed. Bond distances are in angstroms, and bond angles are in degrees.

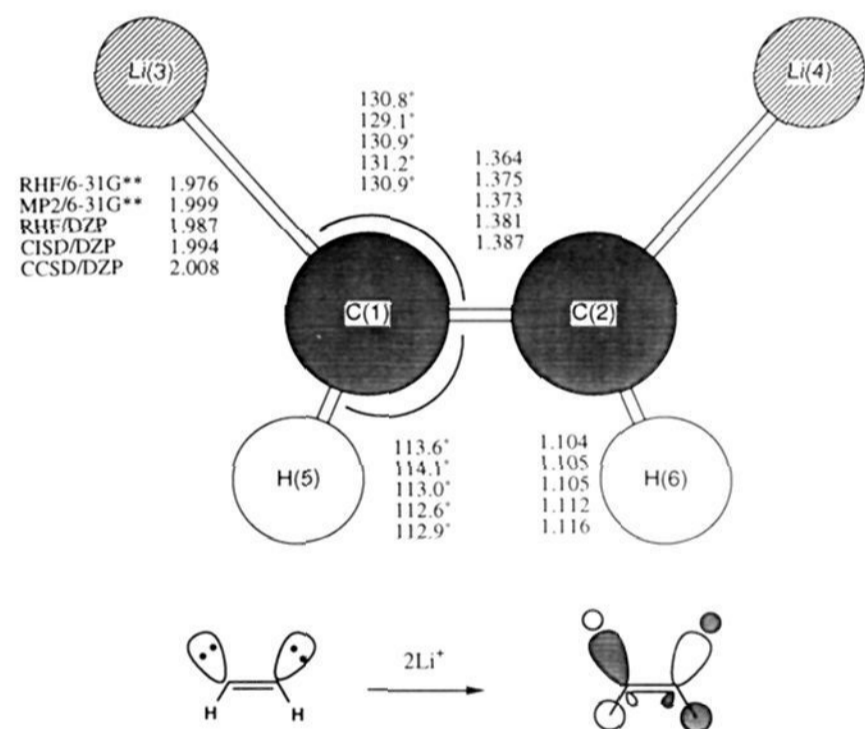


Figure 17. Summary of theoretical geometries for structure **15**, the planar 1A_1 transition state of the *cis*-1,2-dilithioethene molecule that interconverts structure **14a** with its mirror image **14b**, and an electrostatic interpretation with a qualitative representation of the canonical HOMO superimposed. Bond distances are in angstroms, and bond angles are in degrees.

correlation. The T_1 diagnostic has been shown^{35,36} to be an indicator of the importance of nondynamical electron correlation. The computed T_1 value for **7**, 0.057, is above the recommended value³⁶ of 0.020. A multireference treatment, therefore, may further increase the relative stability of **7**.

A precursor to Li_2 elimination from $C_2H_2Li_2$, **9**, presents a relative small barrier to Li_2 elimination, 2.6 kcal/mol at CCSD/DZP (+ZPVE). ZPVE-corrected relative energy comparisons of **9**, the dilithium-acetylene complex, and the molecular fragments $Li_2 + HC\equiv CH$ show **9** is lower lying than $Li_2 + HC\equiv CH$ at all levels of theory. Therefore, the path to Li_2 elimination may include a stable intermediate complex.

Of the two *trans* minima **1** and **7**, **1** is clearly more stable and may be related to the species prepared by MGD.⁹ However, the

(35) Lee, T. J.; Rice, J. E.; Scuseria, G. E.; Schaefer, H. F. *Theor. Chim. Acta* **1989**, *75*, 81-98.

(36) Lee, T. J.; Taylor, P. R. *Int. J. Quantum Chem.* **1989**, *S23*, 199-207.

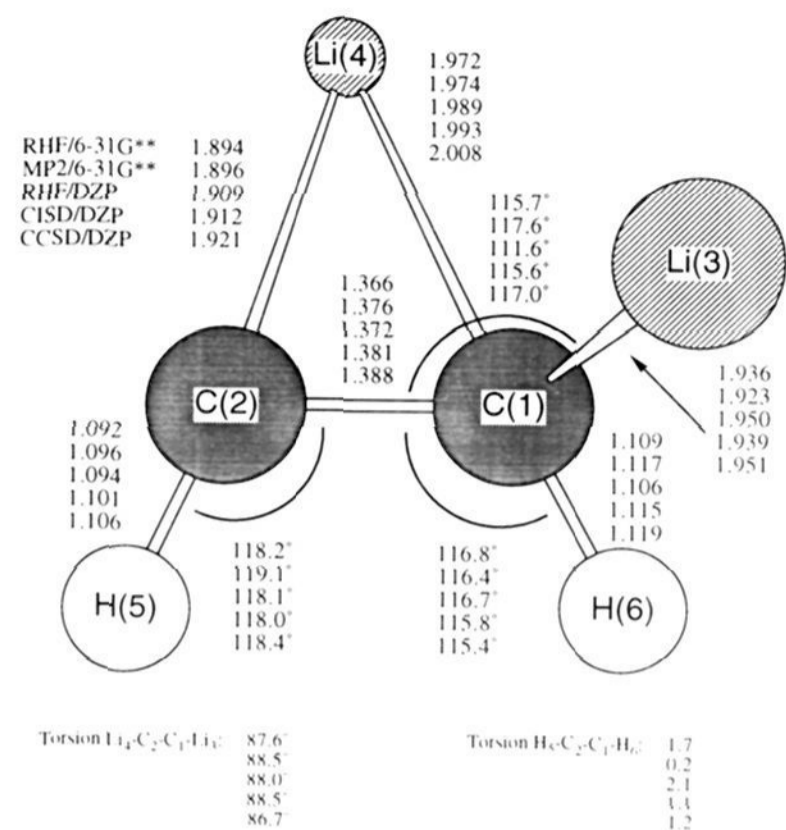


Figure 18. Summary of theoretical geometries for structure **16**, the 1A transition state of the *cis*-1,2-dilithioethene molecule that interconverts structures **11** and **14**, and an electrostatic interpretation with a qualitative representation of the canonical HOMO superimposed. Bond distances are in angstroms, and bond angles are in degrees.

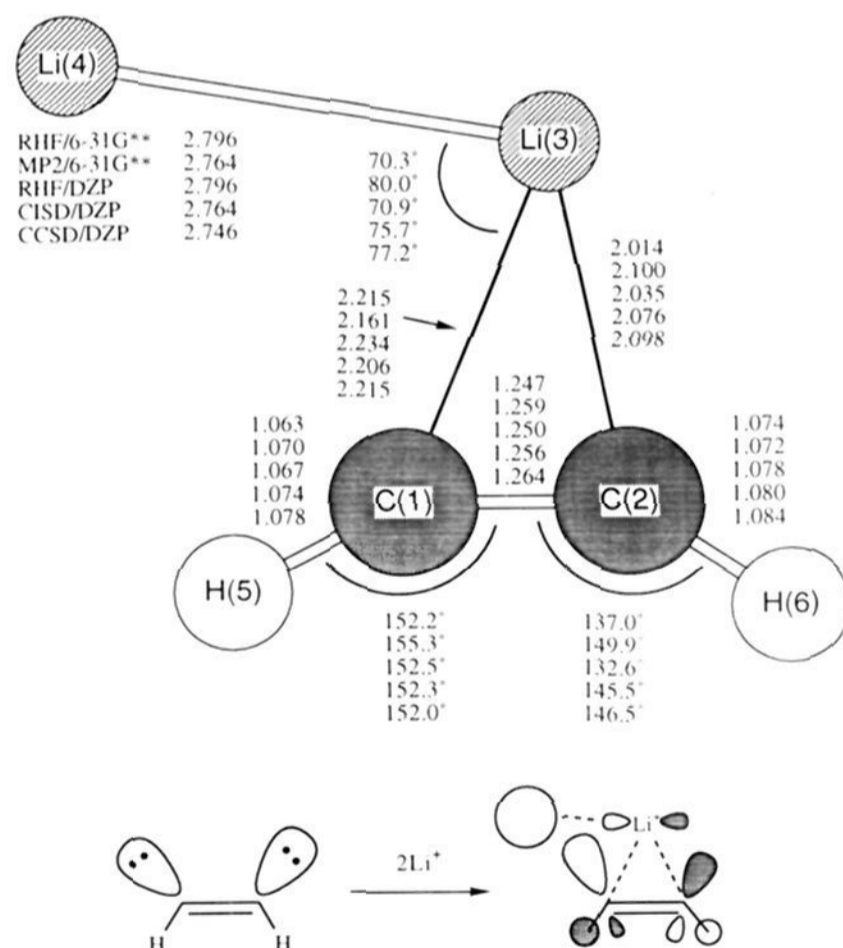


Figure 19. Summary of theoretical geometries for structure **17**, the planar $^1A'$ transition state that interconverts structures **9** and **14**, and an electrostatic representation with a qualitative representation of the canonical HOMO superimposed. Bond distances are in angstroms, and bond angles are in degrees. See the text for an explanation of why the Li(4) atom in the sketch looks different from that in the sketches for the other structures.

experiments refer to aggregates. The rearrangement paths for **1** show *trans* to *cis* arrangement (**1** → **3**) to be as favorable as elimination of Li_2 (**1** → **9**). However, both *trans* to *cis* rearrangement and Li_2 elimination have significantly higher

barriers than rearrangement of **1** to the $C_2H_2Li_2$ global minimum (**1** \rightarrow **11**). MGD did not report *trans* to *cis* rearrangement or Li_2 elimination, lending some support to our theoretical results.

The three *cis* minima **3**, **5**, and **14** are closer in energy than the *trans* minima, with **3** and **14** higher lying than **5** by 8.3 and 4.2 kcal/mol, respectively, at CCSD/DZP (+ZPVE).

The energy barriers for the **3** \rightarrow **5** and **14** \rightarrow **5** rearrangements are small, 3.5 and 2.7 kcal/mol, respectively, at CCSD/DZP (+ZPVE). Conversely, the **5** \rightarrow **3** and **5** \rightarrow **14** barriers are considerably larger, 11.8 and 6.9 kcal/mol, respectively, at CCSD/DZP (+ZPVE). Rearrangements of **3** and **14** to **5** are, therefore, much more favorable than the reverse paths.

Comparison of *cis* and *trans* pathways reveal an interesting peculiarity. One is not likely to isolate a *cis* or *trans* product from a *cis* or *trans* rearrangement, since **11** can be formed via a lower barrier.

Our results for isolated molecules do not include the effects of aggregation. Hence, direct comparison with the experimental results is compromised, although there is agreement in the general features of these results.

Conclusions

Both ethylenic and acetylenic structures exist on the singlet $C_2H_2Li_2$ PES. The global minimum on the $C_2H_2Li_2$ PES is **11**, a planar, acetylenic, C_s symmetry structure that may be viewed as a complex between $HC\equiv CLi$ and HLi . In light of several previous theoretical and experimental studies, it is remarkable that structure **11** had never been suggested, much less characterized. The lowest lying singlet 1,2-dilithioethene structure is *trans*

1. However, *cis* **5** is only 0.1 kcal/mol higher lying at CCSD/DZP (+ZPVE). The energy ordering of the remaining singlet 1,2-dilithioethene minima is **14**, **9**, **3**, and **7**, 4.3, 4.4, 8.4, and 19.4 kcal/mol higher lying than **1** at CCSD/DZP (+ZPVE), respectively.

Evaluation of the bonding interactions through examination of the canonical occupied molecular orbitals and natural bonding analyses shows that while the C-Li interactions involve π interactions, ionic interactions predominate.

Acknowledgment. We would like to acknowledge discussions with Professor Michael Klein. E.E.B. would like to thank Doug R., Christine B., and Bonita J. for their interest and encouragement and Peter S. and Horst S. for translation and patient answers to questions. This research was supported by the U.S. Air Force Office of Scientific Research under Grant No. AFOSR-92-J-0047.

Supplementary Material Available: Theoretical energies, dipole moments, and harmonic vibrational frequencies and IR intensities for structures **1**–**17** (Tables A–Q, respectively) at the RHF/6-31G**, MP2/6-31G**, RHF/DZP, CISD/DZP, and CCSD/DZP levels of theory along with a table containing the Davidson-corrected energies (CISD+Q/DZP) and the CCSD(T)/DZP/CCSD single point energies for structures **1**–**17** and the combined molecular fragments $LiH + LiC\equiv CH$ and $Li_2 + HC\equiv CH$ (Table R) (18 pages). This material is contained in many libraries on microfiche, immediately follows this article in the microfilm version of the journal, and can be ordered from the ACS; see any current masthead page for ordering information.